

SLURRY EROSION IN COMPLEX FLOWS: EXPERIMENT AND CFD

L.J.W. GRAHAM, D. LESTER AND J. WU

CSIRO Materials Science and Engineering, Highett, Victoria 3190, AUSTRALIA

ABSTRACT

Previous erosion research has used sophisticated geometric scanning equipment such as laser and physical probe profilers to examine very small scale erosion scars in fundamental studies. It is also possible to use advanced metrology technology such as 3D laser scanners or coordinate measuring machines for larger scale erosion research in devices of engineering interest. This paper provides experimental results using a coordinate measuring machine (CMM) to directly measure the erosion of a pipe elbow and a flow with a more complex geometry, a cylinder placed in cross flow within a pipe extending from the pipe wall to the centreline of the pipe. In both cases a quantitative map of the erosion was obtained which is suitable for use in comparing with CFD modelling. The CMM results were also compared qualitatively with paint modelling and visual inspection with good agreement. The cylinder in pipe case illustrated a more complex flow pattern with a horseshoe vortex formed at the intersection of the cylinder and pipe wall being manifested in the measured erosion. The CMM data were also compared with CFD for both flow geometries, yielding good qualitative agreement with the potential for quantitative comparisons with CFD erosion modelling as CFD techniques improve.

INTRODUCTION

Surface erosion of materials by solid particle impact is a major problem in many types of industrial equipment involving multiphase flow, due chiefly to the uneven distribution of erosion over the equipment material surface. Erosion localisation, such as pitting and/or holes leads to functional failure, despite the fact that the remainder of the equipment is relatively undamaged. Due to energy arguments, it is often difficult to reduce the average erosion over a particular device, however it is advantageous to alter the erosion distribution such that it is more evenly spread out, thereby significantly increasing the serviceable life of the equipment. This may be achieved by altering the flow geometry within the equipment such that the fluid flow field, and in turn the particle impact dynamics are changed. As the local erosion rate is generally considered to chiefly be a function of the local particle impact rate, velocity and impact angle (Finnie (1960), Laitone (1979), Humphrey (1990), Finnie (1994), Omote et al. (1995), Zhang et al. (2000)), the distribution of local erosion rate is highly dependant upon these dynamics.

To achieve erosion reduction via the approach above, it is necessary to determine the changes in the erosion distribution as a function of any geometrical modifications. Computational Fluid Dynamics (CFD), in

conjunction with erosion models is a useful tool which has been used by many authors to quantitatively predict the erosion distribution generated by various flows for particular material/impact particle combinations. Brown (2002) states that a localised hole was being worn through the steel blanks inside tee-junctions in slurry pipelines at ALCOA's alumina refinery in Western Australia within as short as 13 weeks of operation. Upon determination that the erosion pattern correlated with calculated particle motion using CFD, a new design was devised which exhibited significantly reduced erosion rates. An erosion model was not used in this case. Weetman (1998) uses CFD simulation to redesign the blade geometry along an aerofoil section of an axial flow impeller, resulting in a modified velocity distribution and hence a significantly reduced wear rate.

Despite such success of CFD modelling, it is well recognised that there still exists a strong need for experimental erosion data; for validation of CFD predictions, for development and validation of erosion models, and for assessment of the new design concepts. Whilst there is no lack of experimental erosion data Mishra et al. (1998), Deng et al. (2005), most data reported are in the form of weight loss of samples and photographs of erosion damage patterns. Of significantly greater use are quantitative erosion distribution measurements which capture the actual erosion rate distribution over the material surface and so may be directly compared with CFD predictions. Although rare, there exist some such results in the literature including erosion data such as Chen et al. (2006) through a pipe elbow and a plugged tee obtained using a profiler, and paint erosion modelling described in (Parslow et al. (1997), Parslow et al. (1999), Noui-Mehidi et al. (2008), Wu et al. (2005)) which gives a visual indication of the erosion distribution. However, these techniques are limited in that they are only semi-quantitative or are limited to simple geometries which do not reflect complex industrial equipment. As such, there exists strong demand for experimental techniques which are capable of generating accurate, high (spatial) resolution measurements of erosion over complex geometries as encountered in industrial equipment and devices.

Advanced metrology instrumentation such as surface imaging profilometry is capable of addressing these needs, but thus far has been restricted to examining wear scar details on small test coupons rather than on lab scale flow geometries with sizes meaningful for industrial equipment. Chen, et al. (2006) report data using a profiler to compare the relative erosion rates of a pipe elbow and a plugged tee experimentally and against CFD modelling. Wang et al. (2009) uses surface profilometry and weight loss measurements of jet impingement wear over a variety of materials and compares results with CFD modelling.

The problem with these methods is that the profilometry techniques used are only suited to small and simple geometries. In this study we investigate methods to accurately quantify the erosion rate over complex and/or large-scale geometries and apply these to erosion experiments performed upon two complex geometries. These results are compared with CFD predictions of erosion using standard erosion models in one case as well as paint modelling in the other.

Two possible candidates were found for quantitative erosion distribution measurements on full or laboratory scale slurry handling equipment; a coordinate measuring machine (CMM) which uses a physical probe to map the material surface, and a 3D laser scanner which images and uses triangulation to map the material surface. Inquiries with a provider of metrology services suggested that the CMM had a better resolution than the laser scanner, 5 micron versus approx 100 micron, so the laser scanner is better suited to quite large ($\sim > 1\text{m}$) geometries and erosion damage of at least 1 mm for reasonable resolution. The present contribution details the experiences in using a CMM in slurry erosion measurements where some degree of flow complexity is present. Accurate measurements using this technique on two flow geometries are presented. Corresponding CFD results utilizing accepted erosion models are also presented for comparison purposes in one case and paint erosion modelling used for comparison in the other case. As far as the authors know this is the first report of a CMM used in slurry erosion research although recently Blunt et al. (2009) used a coordinate measuring machine to examine the wear of artificial joints such as knees and hips which have a complex surface geometry.

EXPERIMENTAL DETAILS

The erosion test rig consisted of a 3000 L agitated tank, Warman 3x2 slurry pump, Emerson magnetic flowmeter and associated pipe work (53 mm ID). The samples were arranged so that a vertical flow was presented to them so that stratification effects were eliminated. A schematic of the rig is shown in Figure 1. The working suspension was water with 7% by volume of silica sand (Garfield sand) with a d_{50} of approximately 200 micron.

Two flow geometries were used:

A 1.5x diameter pipe elbow

A bluff body extending over half a pipe diameter in cross flow

The pipe elbow was made from two aluminium blocks, each machined out to make a cavity of half the pipe elbow thus allowing access for the CMM as well as for spray painting for paint erosion modelling as per Noui-Mehidi, et al. (2008) and Wu, et al. (2005). They were then bolted together to make a complete pipe elbow. A photograph of the blocks is shown in Figure 2

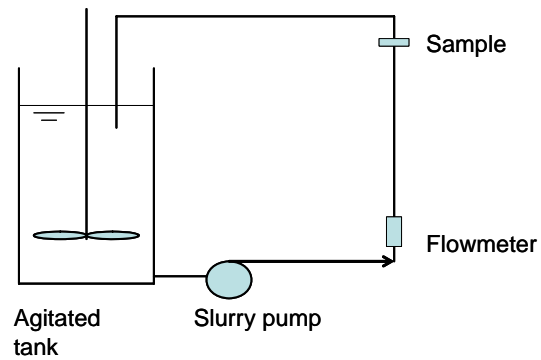


Figure 1. Schematic of pipe loop erosion test rig.



Figure 2. CNC machined aluminium elbow sections. This is a benchmark standard 1.5D elbow. Pipe diameter is 53mm.

The bluff body was a cylinder arranged to protrude to half way through the pipe as shown in Figure 4. The model consisted of an aluminium block with a semi-cylindrical cavity machined out to an internal diameter of 53 mm. A 16 mm cylinder was pressed in near one end of the cavity. A matching aluminium block was machined to provide a full pipe but without the cylinder. The complete block could then be bolted to standard 50 mm pipe flanges on the end of straight pipe lengths located in the erosion test rig. Both models were oriented such that the entry flow was vertical thus eliminating the effects of stratification. The initial dimensions of the models were measured using a Sheffield Discovery II D-8 coordinate measuring machine (CMM). This had a repeatability of measurements within $5\ \mu\text{m}$ as determined during tests as shown in Figure 3 and was significantly superior for the present requirements than the laser scanner initially considered (which has about $100\ \mu\text{m}$ repeatability). This means that the erosion be minimised and yet still measured reducing the effect of geometry change.

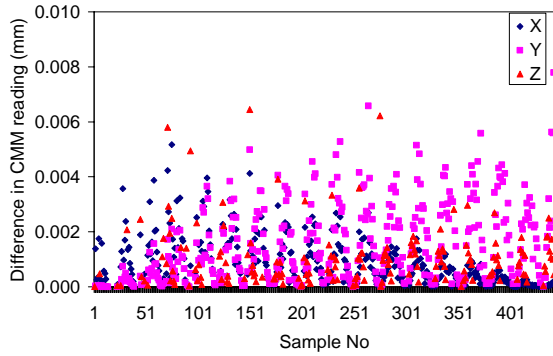


Figure 3. Results of repeatability test of CMM for X, Y and Z coordinates.

The model was then eroded in the slurry erosion rig and the measurements using the CMM repeated. The vector difference between the before and after measurements was then calculated and imported into Tecplot for visualisation. The erosion rate was calculated by dividing the measured erosion in length units by the known time of exposure to the erosion and multiplying by the density of aluminium to give the erosion rate in $\text{kg m}^{-2} \text{s}^{-1}$.



Figure 4. Photograph of flow geometry for erosion tests. Pipe inside diameter was 53mm. Arrow shows the flow direction.

For the pipe elbow case the CMM results are compared with a paint modelling experiment. This erosion measurement technique uses layers of paint as an analogue to the metal surface. Using different colours of paint provides a rapid qualitative visualisation of the erosion distribution. Further details of the paint modelling technique are given in Parslow, et al. (1997), Parslow, et al. (1999), Noui-Mehidi, et al. (2008) and Wu, et al. (2005).

COMPUTATIONAL MODELLING

The commercial CFD code ANSYS CFX[®] was used to calculate the fluid velocity field, particle trajectories and consequent erosion for the cylinder in pipe case. As the erosion experiments were performed in a dynamical regime where the approximation of one-way coupling between the fluid and particle phases is valid, this approximation was employed in the calculations such that

the fluid velocity field without particles is solved first, followed by Lagrangian particle tracking as a subsequent run with the fluid equations switched off. The steady-state non-buoyant incompressible flow field was solved using a 3D unstructured mesh, with a $k-\epsilon$ turbulence model under the assumption that both the inlet velocity field and particle distribution were both uniform 5 pipe diameters upstream of the sample. Particle tracking was performed using the standard transport model in CFX with turbulent dispersion, and 500,000 particles were released in random uniform distribution at the inlet at zero-slip velocity. Brief studies were performed regarding changes of the flow field and erosion predictions with mesh resolution and particle number respectively, and both were shown to be independent. After impact particles are removed from the simulation. Both the Finnie (1960) and the Grant and Tabakoff (1975) models are used to predict the local erosion rate E as a function of the particle impact rate m , velocity v and angle α based upon empirical correlations. The Finnie model is of the form

$$E = m v^n f(\alpha),$$

where n is an empirical coefficient, such that $n=1.8-2.3$ for ductile materials, $n=2.0-4.0$ for brittle materials, and f is a dimensionless wear function

$$f(\alpha) = f_0 \begin{cases} \frac{1}{3} \cos(\alpha)^2 & \text{if } \tan(\alpha) > \frac{1}{3} \\ \sin(2\alpha) - 3\sin(\alpha) & \text{if } \tan(\alpha) \leq \frac{1}{3} \end{cases}$$

where the parameter f_0 scales the rate of erosion. The Grant and Tabakoff model is of the form

$$E = m(k_1 v^2 f(\alpha) \cos^2(\alpha)(1 - R_T^2) + k_3 (v \sin \alpha)^4)$$

where

$$f(\alpha) = \left[1 + k_2 k_{12} \sin\left(\frac{\pi\alpha}{2\alpha_o}\right) \right]^2,$$

$$R_T = 1 - k_4 v \sin \alpha,$$

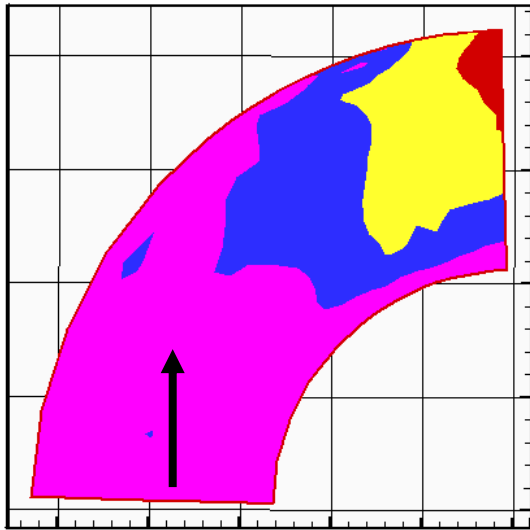
$$k_2 = \begin{cases} 1 & \text{if } \alpha < 2\alpha_o \\ 0 & \text{if } \alpha \geq 2\alpha_o \end{cases}$$

The parameters in the Grant and Tabakoff model were set to those recommended in the CFX manual for sand particles eroding aluminium.

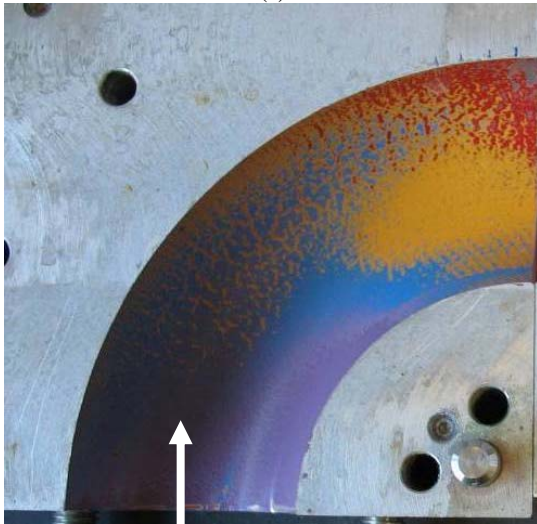
RESULTS AND DISCUSSION

Figure 5a shows the erosion on the aluminium 1.5D elbow model as measured using the CMM with the corresponding paint modelling results shown in Figure 5b. The colour map of the CMM results has been selected to approximate the paint colours used in the paint modelling experiment. It can be seen that both methods give similar results with most erosion occurring for this case towards the exit of the elbow.

The erosion in the more complex flow, the cylinder in pipe, is shown in Figure 6. The results show the maximum erosion occurred on the pipe wall in the immediate vicinity of the cylinder as well as on the top part of the cylinder itself. The erosion just in front of the cylinder may have been underestimated due to the lack of access for the CMM probe. For future tests it would be possible to make the cylinder removable to allow for better access.



(a)



(b)

Figure 5. Measured erosion map of the aluminium elbow averaged over both halves of the model (a); paint modelling result (b). Arrows show flow direction.

The CFD erosion results using the Grant and Tabakoff model are shown in Figure 7. The CFD results agree qualitatively with the experimental results however quantitatively the erosion at the top of the cylinder is less than for the experimental case. However the default erosion model coefficients for aluminium and silica sand have been used, as quoted in the CFX manual, which take no account of the actual aluminium alloys and sand used in the experiments. The CFD results also take no account of the geometry change during the erosion process which may increase or decrease the erosion rate once started. In view of this, the quantitative agreement is quite reasonable.

The erosion calculations using the Finnie model shown in Figure 8 are not scaled into quantitative units as the default model in CFX was used however the qualitative agreement between the Finnie model and the experimental results is good.

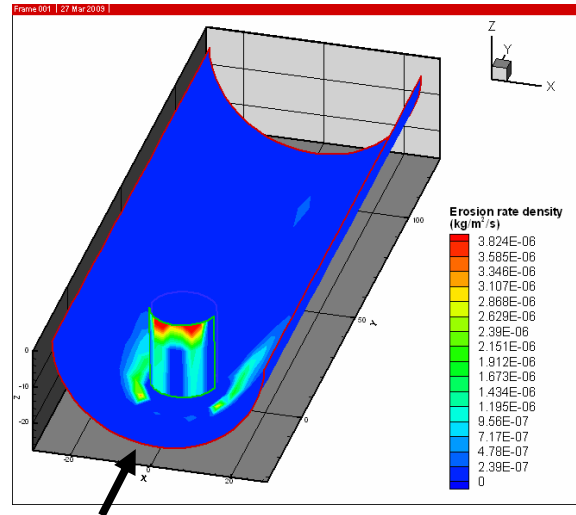


Figure 6. Measured erosion map of the cylinder in pipe flow. Scale is in $\text{kg m}^{-2} \text{s}^{-1}$. Note that the erosion directly in front of the cylinder may be underestimated due to limited access to the physical probe. In future tests the cylinder (or similar parts in other geometries) could be made removable to eliminate this issue. Arrow shows the flow direction.

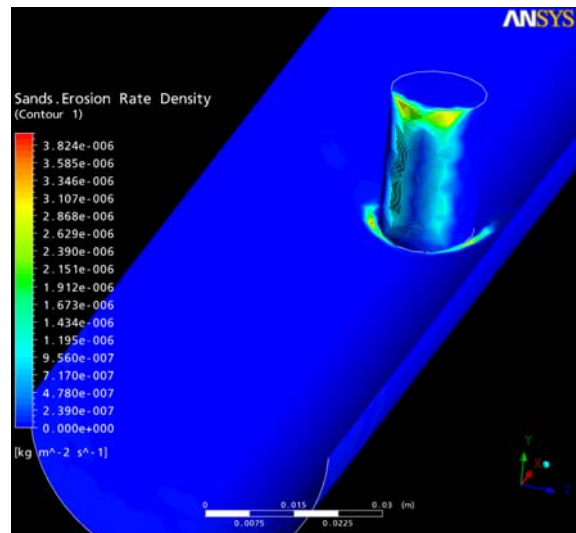


Figure 7. Erosion calculation using Grant and Tabakoff (1975) model.

The erosion is a consequence of the flow field and two views of the erosion as calculated using Grant and Tabakoff (1975) together with streamlines in the vicinity of the erosion on the pipe wall are shown in Figure 9. These streamlines show the commencement of a vortex from the pipe wall-cylinder junction with the vortex extending downstream. Significant erosion is only present near the pipe wall-cylinder junction due to the rapid change of flow direction allowing particle impacts in that region of the flow.

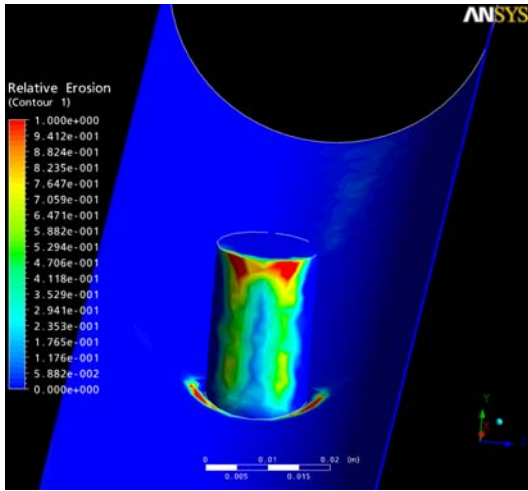


Figure 8. Relative erosion CFD results using default Finnie model in CFX. Note that erosion rate here is not scaled into physical units.

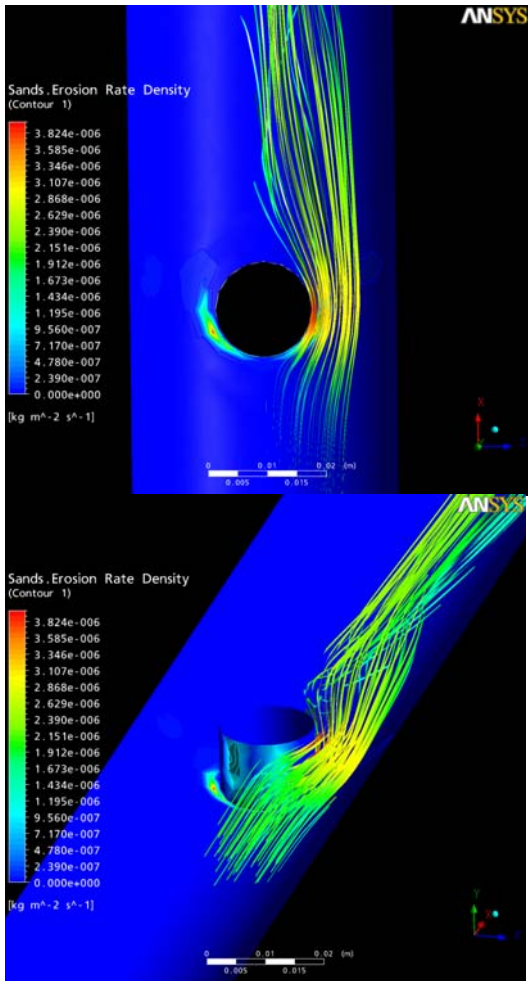


Figure 9. Top and oblique views of erosion calculated using the Grant and Tabakoff (1975) model on the right hand side of each view together with fluid streamlines on the left hand side.

A top view comparison between the CMM results, photograph of the eroded sample and the CFD results using Grant and Tabakoff (1975) is shown in Figure 10. The CMM results correspond well with the photograph; with both experimental methods showing the erosion

in the vicinity of the cylinder/pipe wall junction. The CFD results also show good agreement with experiment however the CFD has not resolved the low erosion “tails” further downstream either side of the cylinder.



Figure 10. Top view of the erosion distribution in the cylinder and pipe flow. This shows clearly the effect of the horseshoe vortex. Top is measurement by CMM, middle is photograph of aluminium model after erosion and bottom is CFD prediction using the model of Grant and Tabakoff (1975) at the same scale as the measured erosion in the top figure. Arrows show flow direction.

CONCLUSION

Slurry erosion on two different geometries, a pipe elbow and a cylinder in pipe flow, has been measured using a coordinate measuring machine. Quantitative erosion measurements have been made using a coordinate measuring machine (CMM) and compared with paint modelling, visual observations and CFD erosion modelling. The CMM data showed good agreement with the paint modelling and visual observations for a pipe elbow and a cylinder in pipe flow. Comparison with CFD erosion modelling for the cylinder in pipe flow showed good agreement with the Grant and Tabakoff erosion model considering that the default coefficients for an aluminium/silica sand system were used rather than values obtained experimentally for the exact sand and aluminium alloy used in the experiments.

The CMM technique shows significant promise for obtaining quantitative data for comparison with CFD modelling of erosion. The technique can be used for full scale equipment if a sufficiently large CMM is available e.g. CMMs with travels of 2000 mm are commercially available. Alternatively if larger items are used with correspondingly larger erosion the laser scanners would become feasible options. Even if the configuration does not allow for measurement access over the whole device of interest, sufficient measurements could be made to provide useful data for comparison with modelling.

ACKNOWLEDGEMENTS

The authors are grateful for the support of Alcoa World Alumina, BHP Billiton / Worsley Alumina, Rio Tinto Alcan and Tyco Flow Control that sponsored this work through the AMIRA International collaborative research project P931 entitled "Reduced Erosion in Multiphase Flow Equipment".

REFERENCES

- BLUNT L., BILLS P., JIANG X., HARDAKER C. and CHAKRABARTY G., (2009). "The Role of Tribology and Metrology in the Latest Development of Bio-Materials", *Wear*, **266**, 424-431.
- BROWN G. J., (2002). "Erosion Prediction in Slurry Pipeline Tee-Junctions", *Applied Mathematical Modelling*, **26**, 155-170.
- CHEN X. H., MCLAURY B. S. and SHIRAZI S. A., (2006). "Numerical and Experimental Investigation of the Relative Erosion Severity between Plugged Tees and Elbows in Dilute Gas/Solid Two-Phase Flow", *Wear*, **261**, 715-729.
- DENG T., LI J., CHAUDHRY A. R., PATEL M., HUTCHINGS I. and BRADLEY M. S. A., (2005). "Comparison between Weight Loss of Bends in a Pneumatic Conveyor and Erosion Rate Obtained in a Centrifugal Erosion Tester for the Same Materials", *Wear*, **258**, 402-411.
- FINNIE I., (1960). "Erosion of Surface by Solid Particles", *Wear*, **3**, 87-103.
- FINNIE I. (1994) Some Reflections on the Past and Future of Erosion. In: 8th International Conference on Erosion by Liquid and Solid Impact (ELSI VIII), Cambridge, England, Sep 04-08.
- GRANT G. and TABAKOFF W., (1975). "Erosion Prediction in Turbomachinery Resulting from Environmental Solid Particles", *J Aircr*, **12**, 471-478.
- HUMPHREY J. A. C., (1990). "Fundamentals of Fluid Motion in Erosion by Solid Particle Impact", *Int J Heat Fluid Flow*, **11**, 170-195.
- LAITONE J. A., (1979). "Erosion Prediction near a Stagnation Point Resulting from Aerodynamically Entrained Solid Particles", *J Aircr*, **16**, 809-814.
- MISHRA R., SINGH S. N. and SESHADRI V., (1998). "Study of Wear Characteristics and Solid Distribution in Constant Area and Erosion-Resistant Long-Radius Pipe Bends for the Flow of Multisized Particulate Slurries", *Wear*, **217**, 297-306.
- NOUI-MEHIDI M. N., GRAHAM L. J. W., WU J., NGUYEN B. V. and SMITH S., (2008). "Study of Erosion Behaviour of Paint Layers for Multilayer Paint Technique Applications in Slurry Erosion", *Wear*, **264**, 737-743.
- OMOTE T., MORITA H. and HIROSE A. (1995) Interaction between Impingement Angles and Materials on Sand Erosion. In: 27th Inter SAMPE Tech Conf.
- PARSLOW G. I., STEPHENSON D. J., STRUTT J. E. and TETLOW S., (1997). "Paint Layer Erosion Resistance Behaviour for Use in a Multilayer Paint Erosion Indication Technique", *Wear*, **212**, 103-109.
- PARSLOW G. I., STEPHENSON D. J., STRUTT J. E. and TETLOW S., (1999). "Investigation of Solid Particle Erosion in Components of Complex Geometry", *Wear*, **233-235**, 737-745.
- WANG M. H., HUANG C. U., NANDAKUMAR K., MINEV P., LUO J. and CHIOVELLI S., (2009). "Computational Fluid Dynamics Modelling and Experimental Study of Erosion in Slurry Jet Flows", *Int J Comput Fluid Dyn*, **23**, 155-172.
- WEETMAN R. J., (1998). "Computer Simulation Helps Increase Life of Impeller in Alumina Hydrate Precipitation from 2 to 8 Years", *J Mater Eng Perform*, **7**, 491-494.
- WU J., NGYUEN B., GRAHAM L., ZHU Y., KILPATRICK T. and DAVIS J., (2005). "Minimizing Impeller Slurry Wear through Multilayer Paint Modelling", *Can J Chem Eng*, **83**, 835-842.
- ZHANG Y., CHENG Y. B. and LATHABAI S., (2000). "Erosion of Alumina Ceramics by Air- and Water-Suspended Garnet Particles", *Wear*, **240**, 40-51.